Gas-Phase Kinetics of Chlorosilylene Reactions. I. ClSiH + Me_3SiH: Absolute Rate Measurements and Theoretical Calculations for Prototype Si−H Insertion Reactions

Rosa Becerra

Instituto de Quimica-Fisica "Rocasolano", C.S.I.C., C/Serrano 119, 28006 Madrid, Spain

Sergey E. Boganov, Mikhail P. Egorov, Valery I. Faustov, Irina V. Krylova, Oleg M. Nefedov, and Vladimir M. Promyslov

N.D. Zelinsky Institute of Organic Chemistry, Russian Academy of Sciences, Leninsky Prospekt 47, 119991 Moscow, Russian Federation

Robin Walsh*

Department of Chemistry, University of Reading, Whiteknights, P.O. Box 224, Reading RG6 6AD, United Kingdom

Received: February 17, 2009; Revised Manuscript Received: March 18, 2009

Time-resolved studies of chlorosilylene, ClSiH, generated by the 193 nm laser flash photolysis of 1-chloro-1-silacyclopent-3-ene, have been carried out to obtain rate constants for its bimolecular reaction with trimethylsilane, Me_3SiH, in the gas phase. The reaction was studied at total pressures up to 100 torr (with and without added SF_6) over the temperature range 297−407 K. The rate constants were found to be pressure independent and gave the following Arrhenius equation: $\log(k/\mathrm{cm^3\ molecule^{-1}\ s^{-1}}) = (-13.97 \pm 0.25) + (12.57 \pm 1.64)\ \mathrm{kJ\ mol^{-1}}/RT\ \ln 10$. The Arrhenius parameters are consistent with a mechanism involving an intermediate complex, whose rearrangement is the rate-determining step. Quantum chemical calculations of the potential energy surface for this reaction and also the reactions of ClSiH with SiH_4 and the other methylsilanes support this conclusion. Comparisons of both experiment and theory with the analogous Si−H insertion processes of SiH_2 and $SiMe_2$ show that the main factor causing the lower reactivity of ClSiH is the secondary energy barrier. The calculations also show the existence of a novel intramolecular H-atom exchange process in the complex of ClSiH with $MeSiH_3$.

Introduction

Silylenes are of importance because they are implicated in the thermal and photochemical breakdown mechanisms of silanes and organosilanes[1] as well as being key intermediates in CVD.[2] Time-resolved studies, carried out in recent years,[3−6] have helped establish a growing database of gas-phase rate constants for these species. While the parent silylene, SiH_2, reacts very rapidly (at close to the collisional rate) with many different molecules, substituted silylenes such as $SiMe_2$ and $SiCl_2$ react more slowly, indicating the significantly deactivating effects of both methyl- and chloro- substitution. Relatively little attention has been paid to the monosubstituted silylenes, XSiH, although we have carried out studies of Si−H insertion reactions for both $MeSiH$[7] and $PhSiH$[8] which showed only small rate reductions for Me and Ph substitution in the silylene. More recently,[9] using a new photochemical precursor, we studied the kinetics of ClSiH with 13 different substrate molecules at room temperature at 10 torr total pressure (in SF_6). Comparisons with reactions of SiH_2 with eight of the same substrates showed a wide variation in relative rate constants, with Cl-for-H substitution producing rate reduction factors of between 2 and 1300. Comparison of an earlier study of ClSiH + SiH_4[10] with that for SiH_2 + SiH_4[11] shows an astonishing rate constant reduction of 75 500.[9]

In this and future papers, we seek to extend ClSiH studies to the investigation of the temperature dependence of its characteristic processes. The present paper concerns the insertion into an Si−H bond. Me_3SiH is the chosen substrate. The work has been augmented by quantum chemical calculations of the structures and energies of the intermediates and transition states involved for reaction of ClSiH with all the methylsilanes, in order to assist with the mechanistic interpretation. There have been no previous studies of ClSiH + Me_3SiH, either experimental or theoretical.

For bookkeeping purposes the subject reactions of this work are

$$\mathrm{ClSiH + SiH_4 \rightarrow ClH_2SiSiH_3} \quad (1)$$

$$\mathrm{ClSiH + MeSiH_3 \rightarrow ClH_2SiSiH_2Me} \quad (2)$$

$$\mathrm{ClSiH + Me_2SiH_2 \rightarrow ClH_2SiSiHMe_2} \quad (3)$$

$$\mathrm{ClSiH + Me_3SiH \rightarrow ClH_2SiSiMe_3} \quad (4)$$

Experimental Section

Rate Measurements. The apparatus and equipment for these studies have been described in detail previously.[11,12] Only essential and brief details are therefore included here. ClSiH was produced by flash photolysis of 1-chlorosilacyclopent-3-ene (CSCP) using a Coherent Compex 100 exciplex laser operating at 193 nm (ArF fill). Photolysis laser pulses (energies ca. 50−70 mJ) were fired into a variable temperature quartz reaction vessel with demountable windows, at right angles to its main axis. ClSiH concentrations were monitored in real time

10.1021/jp901446t CCC: $40.75
Published on Web 04/21/2009

by means of a Coherent Innova 90-5 argon ion laser. The monitoring laser beam was multipassed 36 times along the vessel axis, through the reaction zone, to give an effective absorption path length of ca. 1.5 m. A portion of the monitoring beam was split off before entering the vessel for reference purposes. The monitoring laser was tuned to the 457.9 nm line, coincident with the known transition, $\tilde{A}\ ^1A''(0, 2, 0) \leftarrow \tilde{X}\ ^1A'(0, 0, 0)$, in the ClSiH vibronic band.[13] Light signals were measured by a dual photodiode/differential amplifier combination, and signal decays were stored in a transient recorder (Datalab DL 910) interfaced to a BBC microcomputer. This was used to average the decays of typically five photolysis laser shots (at a repetition rate of 1 Hz or less). The averaged decay traces were processed by fitting the data to an exponential form using a nonlinear least-squares package. This analysis provided the values for the first-order rate coefficients, k_{obs}, for removal of ClSiH in the presence of a known partial pressure of Me_3SiH.

Gas mixtures for photolysis were made up containing 18−30 mtorr of the transient precursor, CSCP, and variable pressures of Me_3SiH. Where pressures were below 10 torr, the total was made up to 10 torr with inert diluent (SF_6). Pressures were measured with capacitance manometers (MKS Baratron).

1-Chlorosilacyclopent-3-ene was prepared as described previously.[9] Me_3SiH (99.5%) was obtained from Fluorochem. Its purity was checked by gas chromatography (GC). All gases used in this work were deoxygenated thoroughly prior to use.

Quantum Chemical Calculations. The electronic structure calculations were performed with the Gaussian 03, revision C.02, software package.[14] The DFT calculations, including the finding and verification of stationary points, were done with the B3LYP functional[15] using the 6-31G(d) basis.[16] All the structures obtained were verified, by examination of their Hessian matrix, as minima (all frequencies real) or transition states (one imaginary frequency). The identities of transition states to particular reactions were established by B3LYP calculations along the minimum energy paths (intrinsic reaction coordinate, IRC) connecting them with local minima. The standard G3(MP2)//B3LYP/6-31G(d)[17] method (denoted G3MP2B3 for short) was employed to determine final energies for all minimum energy species and transition states of interest. For the smaller systems (Si_2ClH_5, Si_2ClCH_7), we also used G3//B3LYP/6-31G(d)[17] (G3B3 for short). For all stationary points, enthalpies at 298 K were also calculated using harmonic oscillator and rigid rotor models.

Results

Kinetic Measurements. It was independently verified during preliminary experiments that, in a given reaction mixture, k_{obs} values were not dependent on the exciplex laser energy (50−70 mJ/pulse routine variation) or number of photolysis shots. Because static gas mixtures were used, tests with up to 10 shots were carried out. The constancy of k_{obs} (five shot averages) showed no effective depletion of reactants in any of the systems. The sensitivity of detection of ClSiH was high but decreased with increasing temperature. Precise concentrations of ClSiH are not known but are not required since the decay kinetics were pseudo-first-order; a rough estimate would be somewhere within the range 0.1−1.0 mtorr (ca. 10^{13} molecule cm^{-3}). Increasing quantities of precursor were required at higher temperatures. However, at any given temperature precursor pressures were kept fixed to ensure a constant (but fairly small) contribution to k_{obs} values, of decay by reaction of ClSiH with precursor. A series of experiments was carried out at five temperatures in the range 297−407 K. At each temperature, a number of runs

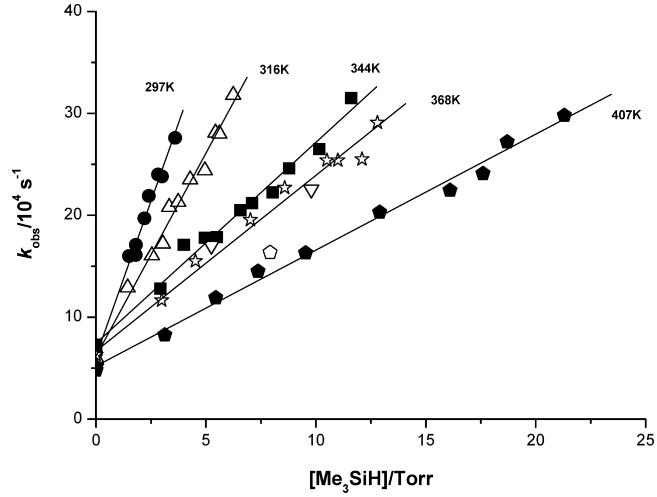

Figure 1. Second-order plots for reaction of ClSiH with Me_3SiH at various temperatures (indicated). Different symbols are used at each temperature. At 368 K, ▽ refers to points where 10 (instead of 5) laser shots were used. At 407 K, ⬠ refers to point with SF_6 added to 30 torr.

TABLE 1: Experimental Second-Order Rate Constants for ClSiH + Me_3SiH

T/K	$k_4/10^{-12}$ cm^3 molecule^{-1} s^{-1}
297.0	1.876 ± 0.065
316.4	1.304 ± 0.041
343.8	0.703 ± 0.025
368.1	0.657 ± 0.029
407.0	0.480 ± 0.013

(at least eight) at different Me_3SiH partial pressures were carried out. The results of these experiments are shown in Figure 1, which demonstrates the linear dependence of k_{obs} on [Me_3SiH], as expected for second-order kinetics. The second-order rate constants, k_4, obtained by least-squares fitting to these plots, are given in Table 1. The error limits are single standard deviations. It should be noted that total pressures are variable in these experiments because of the large amounts of Me_3SiH used (up to 21 torr, 5.0×10^{17} molecule cm^{-3}), although a minimum of value of 10 torr was maintained by addition of SF_6 where necessary. A few experiments with pressures up to 100 torr (SF_6) gave no change in value of k_{obs}, thus showing that the rate constants were not pressure dependent. Because of the increasingly large quantities of Me_3SiH required at higher temperatures, it was decided not to make measurements above 407 K. Figure 2 shows an Arrhenius plot of the rate constants. The resulting equation is

$$\log(k_4/\text{cm}^3\ \text{molecule}^{-1}\ \text{s}^{-1}) = (-13.97 \pm 0.25) + (12.57 \pm 1.64)\ \text{kJ mol}^{-1}/RT \ln 10$$

Uncertainties are again quoted as single standard deviations.

Quantum Chemical Calculations. In order to provide a basis of comparison with experiment, we have undertaken G3MP2B3 calculations on reaction 4. To enhance further our understanding of the effects of methyl substitution in the substrate, we additionally carried out G3MP2B3 calculations on reactions 1−3. To test the reliability of G3MP2B3, we also carried out G3B3 calculations on reactions 1 and 2. The results of these calculations reveal the presence of intermediate complexes and transition states similar to those found in earlier theoretical calculations of silylene insertion reactions.[11,18,19] Apart from the reactants and products, each reaction system possesses one local

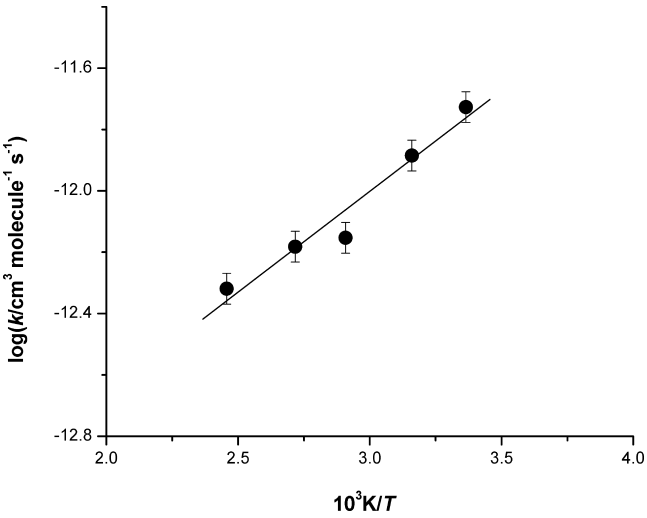

Figure 2. Arrhenius plot for reaction 4 of ClSiH with Me_3SiH.

minimum and at least two transition states. The local minimum, designated **C1**, represents a weakly bound H-bridged complex with chlorosilylene bridging the Si−H bond into which insertion will take place in a *syn* configuration. The transition state **TS1** has the same configuration as **C1**, but transition state **TS2** has a structure with the inserting chlorosilylene in an *anti* configuration with respect to the substrate Si−H bond. It is noteworthy that no complex (**C2**) with the *anti* configuration could be found for any of the reactions. These details are illustrated in Figure 3. The IRC calculations show that the reactions proceed via **C1** and then via either **TS1** or **TS2** to products. It is possible, however, that reactions via **TS2** might occur directly, i.e., without passage through **C1**. In the case of reactions 2 and 3, there is further complexity arising from the different conformational possibilities for the Me groups in the substrates $MeSiH_3$ and Me_2SiH_2. Because these were found to make a negligible difference to the energies of these species (<4 kJ mol^{-1}), they are not shown or discussed in detail in this paper. Only the most stable conformations are considered here. All of the structures are slightly distorted from the symmetrical arrangement of substituents around the Si−Si axis shown in Figure 3, but not enough to affect the descriptions of their structures or of the reaction pathways. There is further complexity because of the chirality of most of the structures, giving rise to right- and left-handed forms. This equally does not affect the mechanistic description. One other transition state, designated **TS3**, was found in the case of ClSiH + $MeSiH_3$ (reaction 2). This transition state has two bridging H atoms and links two conformers of complex **C1**. This is shown in the mechanistic scheme below. **TS3** clearly has a quite different structure from those shown in Figure 3.

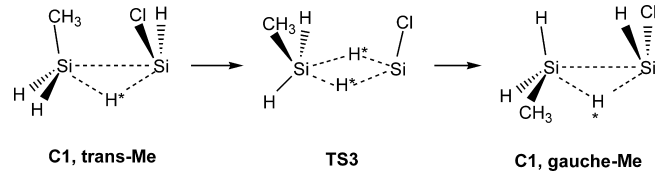

Analogues to **TS3** were not investigated for reactions 1, 3, or 4 (but see later).

The key geometric parameters for the complexes and transition states for all four reactions are given in Table 2. As mentioned above, only data for the most stable conformers are given here (where more than one conformation exists). A number of features of the data are worth pointing out. The complexes, **C1**, all have long central Si···Si bonds, significantly longer than those of the product disilanes (e.g., 2.350 Å for Si−Si in ClH_2SiSiH_3). Si′···H* bonds are significantly longer than Si···H* in all the complexes (Si′ refers to the silicon atom from ClSiH) indicating the rather small extent of H atom transfer. Indeed the Si···H* bond lengths show very little extension (<0.06 Å) compared with the calculated Si−H bond lengths of the reactant silanes (1.486−1.496 Å) The effects of Me-for-H replacement in the substrate silanes produce discernible but only small geometrical effects on the complexes. From SiH_4 to Me_3SiH, the Si···Si decreases by 0.043 Å, the Si−H* bond increases by 0.031 Å, and the Si′···H* bond decreases by 0.161 Å. This shows the gradually increasing extent of H atom transfer with increasing Me-for-H substitution, concomitant with increasing stability (see Table 3).

Geometry changes from complexes to transition states for each reaction pathway are as might be expected. Si···Si bond lengths are significantly reduced by ca. 0.7 Å for **TS1** and 0.9 Å for **TS2**. In the case of **TS2**, they are only just (<0.1 Å) longer than the Si−Si bonds of the product disilanes (2.35−2.36 Å). For **TS1** Si···H* bonds increase by ca. 0.8 Å and Si′···H* bonds decrease by 0.36−0.51 Å, thereby showing a large extent of H atom transfer. Indeed the Si′···H* bonds are scarcely longer (<0.1 Å) than the Si−H bonds in the product disilanes. For **TS2** the extent of H atom transfer is much less marked. Si···H* bonds are 0.20−0.25 Å longer than in **C1**, while Si′···H* bonds are 0.20−0.31 Å shorter than in **C1**, the net effect being that Si···H* are only slightly longer than Si′···H* (<0.16 Å). The Me-for-H substituent effects are not large but do show successive small increases in the extent of H atom transfer between SiH_4 and Me_3SiH.

The energies and enthalpies for the stationary points of all four reactions are given in Table 3 (A referee has raised the question of basis set superposition error (BSSE) in relation to the energies of the complexes. We did not explore this. We believe that the use of composite methods like those employed here (G3MP2B3) largely take account of BSSE. This has been

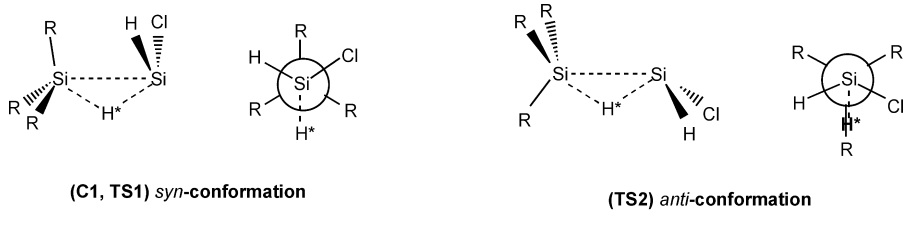

Figure 3. Generic structures of the complexes (local minima) and transition states found by B3LYP/6-31G(d) calculations for the reactions of ClSiH with Me_nSiH_{4-n} ($n = 0-3$). Conformation names are based on the orientation of the ClSiH moiety with respect to the Si−H* bond into which insertion occurs.

TABLE 2: Some Interatomic Distances[a] for Intermediates Formed in Reactions 1−4 Calculated at the B3LYP/6-31G(d) Level

		bond length/Å		
reaction	species	Si···Si′	Si···H*	Si′···H*
(1) ClSiH + SiH_4	**C1**	3.359	1.525	2.003
	TS1	2.612	2.297	1.493
	TS2	2.418	1.718	1.691
(2) ClSiH+$MeSiH_3$	**C1**	3.308	1.539	1.913
	TS1	2.613	2.301	1.489
	TS2	2.423	1.733	1.673
(3) ClSiH + Me_2SiH_2	**C1**	3.326	1.547	1.876
	TS1	2.619	2.374	1.486
	TS2	2.423	1.783	1.648
(4) ClSiH+Me_3SiH	**C1**	3.316	1.556	1.842
	TS1	2.631	2.408	1.483
	TS2	2.450	1.794	1.636

[a] To distinguish the Si atoms, that from the silylene is designated Si′.

shown in other reaction systems.[20,21]), and a generic potential energy surface is shown in Figure 4. A number of features can be discerned. First, the complexes, **C1**, become progressively more stable with increasing methyl substitution. In the same way, the barriers, i.e., the energies of the transition states, are similarly reduced by methyl substitution. Me-for-H replacement stabilizes **C1** by 6−12 kJ mol^{-1}, **TS1** by 2.5−7 kJ mol^{-1}, and **TS2** by 5−13 kJ mol^{-1}. An important finding is that **TS2** is significantly lower than **TS1** by amounts varying between 9 and 20 kJ mol^{-1}. This means that the pathway via **TS2** is always likely to be dominant. The key feature, however, is the fact that for reactions 1 and 2 **TS2** has positive values, while for 3 and 4 it has negative values. Although the energy of **TS2** is not a precise measure of activation energy, it is likely that only the latter two reactions will have negative activation energies. These observations apply whether we consider ΔE(0 K) or ΔH(298 K). Finally, it should be noted that for reactions 1 and 2 the differences between G3B3 and G3MP2B3 are very small (<4 kJ mol^{-1}), thus showing that the two levels of calculation are equally reliable for these reactions.

The ΔE(0 K) and ΔH(298 K) values for **TS3** were calculated to be −6.5 and −9.8 kJ mol^{-1} (G3MP2B3 level). This shows that interconversion of conformations of **C1** for reaction 2 can take place at lower energies than reaction via **TS2**. Although this does not affect the overall process of Si−H insertion studied here, it does suggest that H atom exchange reactions should take place between ClSiH and $MeSiH_3$ faster than insertion.[22]

Discussion

Kinetic Comparisons and General Comments. The main experimental objective of the present study was to measure gas-phase rate constants and Arrhenius parameters for the reaction of ClSiH with Me_3SiH. This has been achieved over the temperature range 297−407 K. The 297 K value ((1.88 ± 0.07) × 10^{-12} cm^3 $molecule^{-1}$ s^{-1}) obtained here compares favorably with our earlier measurement[9] of (1.77 ± 0.11) × 10^{-12} cm^3 $molecule^{-1}$ s^{-1} (299 K). There are no other literature reports of these rate constants or Arrhenius parameters. It is illuminating, however, to compare the data with those of other silylene reactions with Me_3SiH.[7,8,18,23] A comparison of relative rate constants is shown in Table 4 and a comparison of Arrhenius parameters in Table 5. Table 4 shows that at 298 K ClSiH is dramatically less reactive than SiH_2, by a factor of ca. 140, whereas MeSiH and PhSiH are slightly more reactive. Moreover, since ClSiH is even less reactive than $SiMe_2$, this shows that single Cl-for-H substitution in silylene produces a greater rate reduction than two Me-for-H substitutions. At 500 K, all substituted silylenes are less reactive than SiH_2, ClSiH by the impressive factor of 590. Table 5 shows further that for substituted silylenes both *A* factors and activation energies are significantly more negative than those for SiH_2. This is

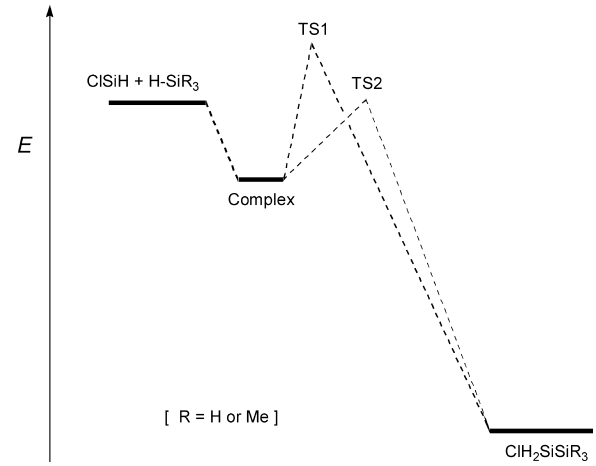

Figure 4. Generic potential energy surface for Si−H insertion reactions of ClSiH.

TABLE 4: Relative Rate Constants[a] for Reaction with Me_3SiH of SiH_2 Compared with Other Silylenes at Two Temperatures

		$k_{rel} = k(SiH_2)/k(SiXY)$			
temp/K	$k(SiH_2)$[b,c]	MeSiH[d]	PhSiH[e]	ClSiH[f]	$SiMe_2$[g]
298	2.55×10^{-10}	0.90	0.65	136	57
500	1.30×10^{-10}	9.8	4.2	590	220

[a] Where necessary, rate constants were calculated from Arrhenius equations. [b] Units: cm^3 $molecule^{-1}$ s^{-1}. [c] Reference 18. [d] Reference 7. [e] Reference 8. [f] This work. [g] Reference 23.

TABLE 3: Electronic Energies[a] (ΔE(0 K)) and Enthalpies[a] (ΔH(298 K)) of Complexes, Transition States, and Products for Reactions 1−4 Calculated at the G2MP2B3 and G3B3 Levels[b]

reactants	quantity	**C1**[c]	**TS1**[c]	**TS2**[c,d]	product
(1) ClSiH + SiH_4	ΔE(0 K)	−10.5 (−12.4)	+26.3 (+28.6)	+17.3 (+15.9)	−171.3 (−174.8)
	ΔH(298 K)	−11.0 (−12.9)	+23.6 (+25.9)	+12.9 (+11.5)	−174.6 (−178.1)
(2) ClSiH + $MeSiH_3$	ΔE(0 K)	−22.3 (−24.4)	+19.3 (+21.4)	+4.0 (+6.1)[d]	−174.9 (−178.5)
	ΔH(298 K)	−22.2 (−24.3)	+17.9 (+19.9)	+0.8 (+3.4)[d]	−176.8 (−180.5)
(3) ClSiH + Me_2SiH_2	ΔE(0 K)	−30.7	+13.6	−4.4	−178.0
	ΔH(298 K)	−30.4	+12.8	−6.7	−179.3
(4) ClSiH + Me_3SiH	ΔE(0 K)	−36.7	+10.8	−9.2	−179.7
	ΔH(298 K)	−36.1	+10.4	−11.2	−180.5

[a] Values in kJ mol^{-1}. [b] G3B3 values are given in parentheses (reactions 1 and 2 only). [c] For reactions 2 and 3, only the most stable conformation is included. [d] For reaction 2, **TS2**, these G3B3 values correspond to a different conformation.

TABLE 5: Arrhenius Parameters for Various Silylene Insertion Reactions with Me_3SiH

reaction	$\log(A/cm^3$ molecule^{-1} s$^{-1})$	E_a/kJ mol^{-1}	ref
$SiH_2 + Me_3SiH$	-10.37 ± 0.10	-4.65 ± 0.76	18
$SiMe_2 + Me_3SiH$	-13.41 ± 0.14	-11.20 ± 1.03	23
$MeSiH + Me_3SiH$	-12.80 ± 0.10	-18.40 ± 0.90	7
$PhSiH + Me_3SiH$	-12.14 ± 0.28	-15.60 ± 2.30	8
$ClSiH + Me_3SiH$	-13.97 ± 0.25	-12.57 ± 1.64	this work

consistent with the now well-established intermediate complex mechanism for Si−H insertion,[3,4,6] viz

$$R_3Si{-}H + SiXY \underset{-a}{\overset{a}{\rightleftharpoons}} R_3Si{-}H \cdots SiXY \overset{b}{\rightarrow} R_3SiSiHXY$$

where R = H or Me; X and Y may be any of H, Me, or Cl.

Both the differences in relative rate constants and in Arrhenius parameters arise because of switches between steps a and b as the slow, rate-determining step for the various silylenes. For the insertion by SiH_2, step a, the encounter or complex-forming process, is the rate-determining step, whereas for the substituted silylenes, it is step b, the complex rearrangement process, which is much slower and significantly affecting the rate, even if not completely controlling it. The transition state for the relatively unhindered association step a will be loose, whereas that for the more encumbered, bond-bridging rearrangement step b will be tight. This accounts in general for the differences in *A* factors. The differences in negative activation energies are determined by the differences in binding energies and rearrangement barriers of the complexes. These are less obvious and indicate the need for theoretical calculations. The results of the theoretical calculations carried out here are discussed in the next section.

A brief comment on the reaction of ClSiH with precursor, CSCP, seems worthwhile. The intercepts of Figure 1 correspond to rate constants in the range $(1.0 \pm 0.3) \times 10^{-10}$ cm^3 molecule^{-1} s^{-1}, assuming complete reaction of ClSiH with CSCP. These values, significantly higher than those for reaction of ClSiH with Me_3SiH, correspond quite closely to that (1.13×10^{-10} cm^3 molecule^{-1} s^{-1}) obtained by us earlier[9] for reaction of ClSiH with $H_2C{=}CHCMe_3$ at 299 K, suggesting that the mechanism is more likely to involve addition to the π-bond of CSCP rather than insertion into its Si−H bond. We have no analytical information on this process, but it seems unlikely that any product of this reaction would interfere with the observed reaction decays.

Quantum Chemical Calculations and the Mechanism. While there have been no previous calculations of the energy surface for reaction 4, calculations of the energy barriers for other Si−H insertion processes of ClSiH have been carried out by Swihart and Carr[24] at a variety of different levels of theory, in particular for reaction 1. Although these workers did not establish the intermediacy of complexes in the reaction, they did obtain a barrier of 20 kJ mol^{-1} (G2 level) for this process, i.e., the insertion of ClSiH into the Si−H bond of SiH_4. This compares favorably with the 17 kJ mol^{-1} found here (Table 3).

Table 6 shows a comparison of the available calculated energies ($\Delta E(0)$) of the Si−H insertion reactions of SiH_2, $SiMe_2$, and ClSiH. It should be borne in mind that the levels of calculation are different for the three silylene species. In spite of this limitation, some reasonable comparisons can be made. There are a number of similarities between the findings of these calculations for ClSiH and those carried out by us previously on the Si−H insertion reactions of SiH_2[18] and $SiMe_2$.[19] All the reactions proceed via intermediate complexes. For all silylenes studied so far (SiH_2, $SiMe_2$, ClSiH), where comparisons are possible, the complexes seem to prefer the *syn* conformation, viz., **C1** is more stable than **C2**. However it should be noted that **C1** complexes could not be found in some of the SiH_2 insertions and **C2** complexes could not be found for the ClSiH insertions, i.e., this study. For the SiH_2 insertions, the secondary barriers (**TS1** or **TS2**) lie barely above the complexes in energy and therefore have little or no effect on the reaction rates. For $SiMe_2$ and ClSiH insertions, the secondary barriers are substantial for all four reactions. **TS1** is much higher in energy that **TS2**. Indeed for ClSiH all four reactions have positive energy values for **TS1**. Thus the secondary transition state clearly prefers the *anti* to the *syn* conformation. This is understandable since the transition states structures are tighter than those of the complexes and the steric hindrance of the *syn* conformation is obviously more severe. For **TS2**, Table 6 shows that ClSiH has higher secondary barriers than $SiMe_2$ by 16 and 13 kJ mol^{-1} in the insertion reactions with SiH_4 and $MeSiH_3$, respectively. There are no values for **TS2** for $SiMe_2 + Me_2SiH_2$ or Me_3SiH to extend the comparison. However, it seems highly likely that differences of a similar magnitude exist between the reactions of ClSiH and $SiMe_2$ with these two silanes. The higher secondary barriers for ClSiH compared with $SiMe_2$ help explain why ClSiH insertion is slower than that of $SiMe_2$ into Si−H bonds. A semiquantitative pictorial representation of the differences between the effective reaction surfaces for the three silylenes with Me_3SiH is shown in Figure 5.

TABLE 6: Comparison of ab Initio Calculated Energies of Stationary Points on the Surfaces for Si−H Bond Insertion of Three Silylenes with Silane and the Methylsilanes

		substrate					
silylene	stationary point	SiH_4	$MeSiH_3$	Me_2SiH_2	Me_3SiH	method	ref
SiH_2	**C1**	−39	−45	−[a]	−[a]	CCSD(T)/ 6-311G(d,p)	18
	TS1	−35	−41	−[a]	−[a]		
	C2	−29	−36	−44	−50		
	TS2	−25	−33	−40	−44		
$SiMe_2$	**C1**	−6	−13	−[b]	−[b]	G2MP2B3	19
	TS1	+17	+11	−[b]	−[b]		
	C2	−6	−[a]	−[b]	−[b]		
	TS2	+1	−9	−[b]	−[b]		
ClSiH	**C1**	−10	−22	−31	−37	G3MP2B3	this work
	TS1	+26	+19	+14	11		
	C2	−[a]	−[a]	−[a]	−[a]		
	TS2	+17	+4	−4	−9		

[a] Species not found. [b] Reaction not investigated.

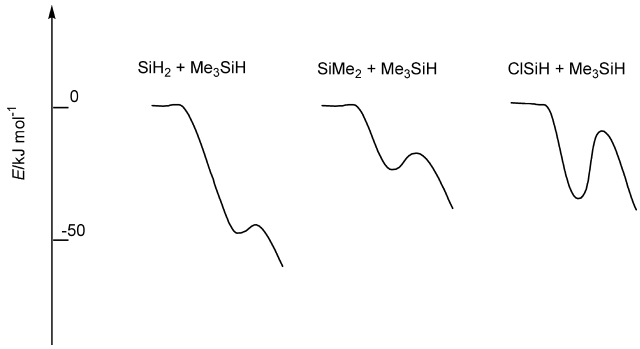

Figure 5. Comparison of calculated energy profiles for reactions of SiH_2, $SiMe_2$, and ClSiH with Me_3SiH. See text for details.

TABLE 7: Room Temperature Rate Constants, Estimated *A* Factors, and Calculated Activation Energies for Reactions of ClSiH with Silane and the Methylsilanes

silane	k(298 K)[a]	log A[a,b]	E_a/kJ mol^{-1}[c]
SiH_4	5.3×10^{-15}[d]	−13.37	+5.17
$MeSiH_3$	3.16×10^{-13}[e]	−13.49	−5.65
Me_2SiH_2	1.43×10^{-12}[e]	−13.67	−10.41
Me_3SiH	1.88×10^{-12}[f]	−13.97	−12.80

[a] Units: cm^3 molecule^{-1} s^{-1}. [b] Estimated values (see text). [c] Calculated (see text). [d] Reference 10. [e] Reference 9. [f] This work.

A strict comparison of the calculations with the negative activation energies of Table 5 is not possible, because, as explained above, the overall activation energies depend on the extent to which step b is rate controlling. This has been discussed in some detail by Becerra and Walsh,[6] who have shown that if **TS2** is more than ca. 34 kJ mol^{-1} below the threshold step a will control the rate, and if it is less than ca.17 kJ mol^{-1} below the threshold step b will control the rate. In between these values both steps will contribute. For ClSiH, with **TS2** at −9 kJ mol^{-1}, step b should be clearly rate controlling, and the observed activation energy of −12 kJ mol^{-1} is pleasingly close to this value.

Although activation energies have not been measured for ClSiH with the other methylsilanes, an approximate idea of their values can be obtained by combining the values of their room temperature rate constants with assumed *A* factors based on the value for ClSiH + Me_3SiH obtained here and corrected only for path degeneracy. These values are given in Table 7. These estimated activation energies show clearly the trend of reducing magnitude with increasing number of methyl groups in the substrate silane. They also show in particular that the activation energy for ClSiH + SiH_4 (reaction 1) is expected to be positive. The values are all a bit lower than those calculated for **TS2**, but the trend is reproduced. Given the assumptions and uncertainties involved in these estimates, this must be regarded as reasonable consistency of theory with experiment.

In general terms, it is understandable that ClSiH should be a less reactive silylene than SiH_2. This is because of the presence of the Cl atom lone pairs which donate to the silicon empty p orbital by $p_\pi-p_\pi$ overlap, thus making ClSiH less electrophilic than SiH_2. However, what is less clear is the extent to which this manifests itself in the binding energies of the intermediate complexes and the heights of the secondary barriers. Thus while the comparison between ClSiH and SiH_2 seems clear enough, viz., ClSiH has more weakly bound complexes with higher secondary barriers, the comparison with $SiMe_2$ is less easy to interpret. $SiMe_2$ has even more weakly bound complexes than ClSiH, but a lower secondary barrier to rearrangement. $SiMe_2$ is known to be stabilized relative to SiH_2,[25] but the effects on the stationary points of Cl-for-H and Me-for-H substitution are opposed. Fortunately one feature of these insertions does remain clear, viz., the trend of complex stabilities and secondary barriers with methyl substitution in the substrate silane. The Si atom in the substrate becomes more electropositive with methyl substitution, due to electron inductive withdrawal (C is more electronegative than Si). This makes the binding of the complex stronger and lowers the secondary barrier, which is associated with the nucleophilic interaction of the lone pair of the inserting silylene.[3,4,6,9] This remains true for all of the silylene Si−H insertion reaction sequences that have been investigated quantitatively so far.

Although not part of the main thrust of this paper, the finding of **TS3** for reaction 2 involving the exchange of H atoms between ClSiH and $MeSiH_3$ is of some interest. Swihart and Carr[24] were the first to obtain theoretical evidence for such processes by finding similar four-center transition states for exchange reactions of the type

$$\mathrm{ClSiH} + \mathrm{SiH}_n\mathrm{Cl}_{4-n} = \mathrm{SiH}_2 + \mathrm{SiH}_{n-1}\mathrm{Cl}_{5-n}$$
$$\mathrm{ClSiH} + \mathrm{SiH}_n\mathrm{Cl}_{4-n} = \mathrm{SiCl}_2 + \mathrm{SiH}_{n+1}\mathrm{Cl}_{3-n}$$

These processes were calculated to have energy barriers several kJ mol^{-1} above the insertion barriers. The difference with **TS3** found here is that its energy lies not only below the reaction threshold but also below **TS2**, the secondary barrier for insertion. This means that this reaction should be fast enough to make it accessible to experimental investigation. To our knowledge, there is as yet no experimental study of such a process.

Thermochemical Considerations. There are, unfortunately, no experimental values to compare with the enthalpy changes calculated here for reactions 1−4. In the case of reaction 1, Swihart and Carr[24] obtained $\Delta H^o(298\ \mathrm{K}) = -186$ kJ mol^{-1} (G2 level) which compares reasonably well with our values of −175 (−178) kJ mol^{-1} (G3MP2B3 (G3B3) levels). Further comparisons are possible with previous enthalpy calculations for the analogous insertion reactions of SiH_2[18] and $SiMe_2$.[19] For SiH_2, values in the range −223 to −225 kJ mol^{-1} (MP2/6-311G(d,p) level) and −209 to −211 kJ mol^{-1} (CCSD(T)/6-311G(d,p) level) were obtained for the insertion reaction analogues of reactions 1−4.[18] For $SiMe_2$ values of −211 and −209 kJ mol^{-1} (G2MP2B3 level) were obtained for the insertion analogues of reaction 1 and 2, respectively.[19] Comparison with the values calculated here (Table 3) suggests that the ClSiH insertion reactions are ca. 40 ± 10 kJ mol^{-1} less exothermic than those of SiH_2 and ca. 35 kJ mol^{-1} less exothermic than those of $SiMe_2$. Although more than one factor may be at work here, we suspect the major reason for these differences lies in the extra stabilization of the ClSiH (provided by the $p_\pi-p_\pi$ overlap). This would be consistent with the known divalent state stabilization energies (DSSE) of 94 ± 4 and 188 ± 10 kJ mol^{-1} for SiH_2 and $SiCl_2$, respectively.[25] Although a DSSE value for ClSiH has not been evaluated, the extra stabilization of $SiCl_2$ clearly indicates a substantial Cl-for-H increment.

Acknowledgment. S.E.B, M.P.E, V.I.F., I.V.K., O.M.N., and V.M.P thank RFBR (project no. 07-03-00693), the President of the Russian Federation (Presidential program for support of leading research schools, grant NSh-3237.2008.03), and the Russian Academy of Sciences (program OX-01). R.B. thanks the Ministerio de Educacion y Ciencia for support under project CTQ2006-10512.

References and Notes

(1) Gaspar, P. P.; West R. Silylenes. In *The Chemistry of Organosilicon Compounds*; Rappoport, Z., Apeloig, Y., Eds.; Wiley; Chichester, 1998; Vol. 2, Chapter 43, p 2463.

(2) Ho, P.; W. G. Breiland, W. G. *Appl. Phys. Lett.* **1983**, *43*, 125, and references cited therein.

(3) Jasinski, J. M.; Becerra, R.; Walsh, R. *Chem. Rev.* **1995**, *95*, 1203.

(4) Becerra, R.; Walsh, R. Kinetics and Mechanisms of Silylene Reactions: A Prototype for Gas-Phase Acid/Base Chemistry. In *Research in Chemical Kinetics*; Compton, R. G., Hancock, G. Eds.; Elsevier: Amsterdam, 1995; Vol. 3, Chapter 6, p 263.

(5) Safarik, J.; Sandhu, V.; Lown, E. M.; Strausz, O. P.; Bell, T. N. *Res. Chem. Int.* **1990**, *14*, 105.

(6) Becerra, R.; Walsh, R. *Phys. Chem. Chem. Phys.* **2007**, *9*, 2817.

(7) Becerra, R.; Frey, H. M.; Mason, B. P.; Walsh, R. *J. Chem. Soc., Faraday Trans.* **1993**, *89*, 411.

(8) Blitz, M. A.; Frey, H. M.; Tabbutt, F. D.; Walsh, R. *J. Phys. Chem.* **1990**, *94*, 3294.

(9) Becerra, R.; Boganov, S. E.; Egorov, M. P.; Krylova, I. V.; Nefedov, O. M.; Walsh, R. *Chem. Phys. Lett.* **2005**, *413*, 194.

(10) Ho, P.; Breiland, W. G.; Carr, R. W. *Chem. Phys. Lett.* **1986**, *132*, 422.

(11) Becerra, R.; Frey, H. M.; Mason, B. P.; Walsh, R.; Gordon, M. S. *J. Chem. Soc., Faraday Trans.* **1995**, *91*, 2723.

(12) Becerra, R.; Boganov, S. E.; Egorov, M. P.; Faustov, V. I.; Krylova, I. V.; Nefedov, O. M.; Walsh, R. *J. Am. Chem. Soc.* **2002**, *124*, 7555.

(13) Herzberg, G.; Verma, R. D. *Can. J. Phys.* **1964**, *42*, 395.

(14) Frisch, M. J.; Trucks, G. W.; Schlegel, H. B.; Scuseria, G. E.; Robb, M. A.; Cheeseman, J. R.; Montgomery, J. A., Jr.; Vreven, T.; Kudin, K. N.; Burant, J. C.; Millam, J. M.; Iyengar, S. S.; Tomasi, J.; Barone, V.; Mennucci, B.; Cossi, M.; Scalmani, G.; Rega, N.; Petersson, G. A.; Nakatsuji, H.; Hada, M.; Ehara, M.; Toyota, K.; Fukuda, R.; Hasegawa, J.; Ishida, M.; Nakajima, T.; Honda, Y.; Kitao, O.; Nakai, H.; Klene, M.; Li, X.; Knox, J. E.; Hratchian, H. P.; Cross, J. B.; Adamo, C.; Jaramillo, J.; Gomperts, R.; Stratmann, R. E.; Yazyev, O.; Austin, A. J.; Cammi, R.; Pomelli, C.; Ochterski, J. W.; Ayala, P. Y.; Morokuma, K.; Voth, G. A.; Salvador, P.; Dannenberg, J. J.; Zakrzewski, V. G.; Dapprich, S.; Daniels, A. D.; Strain, M. C.; Farkas, O.; Malick, D. K.; Rabuck, A. D.; Raghavachari, K.; Foresman, J. B.; Ortiz, J. V.; Cui, Q.; Baboul, A. G.; Clifford, S.; Cioslowski, J.; Stefanov, B. B.; Liu, G.; Liashenko, A.; Piskorz, P.; Komaromi, I.; Martin, R. L.; Fox, D. J.; Keith, T.; Al-Laham, M. A.; Peng, C. Y.; Nanayakkara, A.; Challacombe, M.; Gill, P. M. W.; Johnson, B.; Chen, W.; Wong, M. W.; Gonzalez, C.; Pople, J. A. *Gaussian 03*, revision C.02; Gaussian, Inc.: Wallingford, CT, 2004.

(15) Becke, A. D. *J. Chem. Phys.* **1993**, *98*, 5648.

(16) Hehre, W. A.; Radom, L.; Pople, J. A. *Ab Initio Molecular Orbital Theory*; Wiley: New York, 1986.

(17) Baboul, A. G.; Curtiss, L. A.; Redfern, P. C.; Raghavachari, K. *J. Chem. Phys.* **1999**, *110*, 7650.

(18) Becerra, R.; Carpenter, I. W.; Gordon, M. S.; Roskop, L.; Walsh, R. *Phys. Chem. Chem. Phys.* **2007**, *9*, 2121.

(19) Becerra, R.; Boganov, S. E.; Egorov, M. P.; Faustov, V. I.; Krylova, I. V.; Nefedov, O. M.; Promyslov, V. M.; Walsh, R. *J. Phys. Chem. A* **2008**, *112*, 849.

(20) Kim, K. H.; Kim, Y. *Theor. Chem. Acc.* **2006**, *115*, 18.

(21) Joshi, R.; Ghanty, T. K.; Naumov, S.; Mukherjee, T. *J. Phys. Chem. A* **2007**, *111*, 2362.

(22) Since the original submission of this paper, we have now found the analogue to **TS3** in reaction 4, the system under experimental investigation. The ΔE(0 K) and ΔH(298 K) values were calculated to be −21.8 and −23.7 kJ mol^{-1} (G3MP2B3 level), respectively.

(23) Baggott, J. E.; Blitz, M. A.; Frey, H. M.; Walsh, R. *J. Am. Chem. Soc.* **1990**, *112*, 8337.

(24) Swihart, M. T.; Carr, R. W. *J. Phys. Chem. A* **1997**, *101*, 7434.

(25) Becerra, R.; Walsh, R. Thermochemistry. In *The Chemistry of Organosilicon Compounds*; Rappoport, Z., Apeloig, Y., Eds.; John Wiley & Sons: New York, 1998; Vol. 2, Chapter 4, p 153.

JP901446T